Consequences of altered *Cacna1c* and *Cacna1d* expression levels on $Ca_V1.2$ and $Ca_V1.3$ activity

---

A thesis submitted in partial fulfillment of the Degree of

Bachelor of Science in Neuroscience with Honors

University of Michigan, Ann Arbor

---

by

Justin McMahon

Co-sponsored by

Geoffrey Murphy, PhD and Richard Hume, PhD

April 1, 2020

Abstract

L-type voltage-gated calcium channels (LVGCCs) play an important role in neuronal excitability. In the brain, $Ca_V1.2$ and $Ca_V1.3$ are the most predominately expressed LVGCCs. Genetic mutations of either of these LVGCCs have been shown to confer impairment in memory consolidation as well as increase risk for development of neuropsychiatric disorders. Therefore, we used *in vitro* calcium imaging to test the role of altered *Cacna1c* or *Cacna1d* expression levels on the underlying calcium dynamics. Additionally, we performed immunocytochemistry (ICC) to localize expression patterns of LVGCCs in hippocampal neuronal cultures. We show that genetic alterations of LVGCC expression levels may result in a potentially reciprocal mechanism of calcium activity. The characterization of $Ca_V1.2$ and $Ca_V1.3$ expression in neuronal cultures allows for future calcium imaging experiments with much higher spatial resolution.

Contents

Scientific Acknowledgements

I have been granted permission by Dr. Victor Cazares, a postdoctoral fellow in our lab, to include preliminary data he collected and analyzed. This data was collected in 2017, prior to my starting in this lab. The person who conducted each illustrated experiment presented in this study is indicated in the table below:

Figure #	Person who was responsible for the illustrated experiment
1	All data in these figures was collected, analyzed, and illustrated entirely by me
2	Dr. Victor Cazares collected and analyzed the data, I have illustrated the figure
3	All data in these figures was collected, analyzed, and illustrated entirely by me
4	All data in these figures was collected, analyzed, and illustrated entirely by me
5	All data in these figures was collected, analyzed, and illustrated entirely by me

Personal acknowledgements

I would like to first acknowledge Lara Ouillette, Master's candidate, for preparing and feeding hippocampal neuron cultures used for calcium imaging experiments. Additionally, I would like to thank Lara Ouillette and Emily Glass, research technician, for their help with genotyping mice used in this study. Without their support and generosity, this study would not have been possible.

Next, I would like to recognize the following lab members for offering guidance throughout the study: Victor Cazares, PhD, for his technological support regarding data analysis software and microscopy, as well as troubleshooting immunocytochemistry experiments; Kasia Glanowska, PhD, for her overall assistance in helping to design a thorough set of experiments; Rachel Parent, M.S., for her advice regarding antibody-use in immunocytochemistry experiments; Shannon Moore, PhD, for her technological support regarding microscopy; Tamara Stevenson, PhD, for her technological support in establishing remote connection for continued data analysis during the COVID-19 pandemic.

Lastly, for social support throughout my time at the University of Michigan, I would like to thank my parents: Lisa McMahon, mother, Michael McMahon, father, and Shannon McMahon, stepmother. I also extend my gratitude to friends Lauren Lee, B.S. candidate in Sports Medicine and Applied Music – Cello Performance at Pepperdine University, and Anna Patterson, B.S. candidate in Neurobiology at the University of Wisconsin-Madison, for their social support while composing this thesis.

Introduction

General Overview

Neuroscience is the study of the nervous system and its structural, biological, chemical, and psychological components. These components work together cohesively in order for us to perceive information and interact with our environment. In the human body, the brain and spinal cord make up the central nervous system – while the peripheral nervous system is composed of the nerves that branch out from the spinal cord to organs and muscles throughout the body. With the increasing popularity of neuroscience, research projects range from the discovery of individual proteins in mice to more translational initiatives such as behavioral studies of humans with neuropsychiatric disorders. These research projects work to develop our understanding of fundamental biological mechanisms which underpin daily human function. More than this, they strive to develop cutting-edge therapeutics which improve quality of life for neurologically impaired individuals across the globe. How is it that this tremendous goal of developing novel treatments for neurological disorders is being achieved? The story of therapeutic research is one which starts far before the onset of clinical trials.

Beginning with an idea, a group of scientists design a plan to answer a question. An appropriate animal model is selected to investigate based on the phenotype of interest. A phenotype refers to the observable characteristics of an organism caused by its genetics and surrounding environment. For instance, this could be a specific disease or malformation caused by an underlying genetic mutation. While the most scientifically ideal scenario would be to answer questions about these phenotypes based on experimental results in humans, the ethical component of science must be taken into consideration. As such, we commonly use animals – such as mice, rats, fruit flies, monkeys, or zebrafish – to model the specific mechanism we are interested in studying. Because a neuron functions similarly in humans and mice, we are often able to successfully study aspects of neuronal function without ever interfering with a human's nervous system. Furthermore, *in vitro* culturing cells (that is, growing cells in a controlled artificial environment) in a dish has proven to be an effective strategy for studying physiological principles, given the easily controllable environment and genetic homogeneity among the cells within the culture. To fully comprehend the abstract idea of why looking at cells in a dish is

important for studying disorders like schizophrenia or bipolar disorder, we must look at the underlying biology.

In the field of neuropsychiatric disorders research, it is important to understand fundamental neuroscience principles when comprehending the implications of altered protein expression levels due to genetic mutations. There are approximately eighty-six billion neurons in the human brain, connected in meaningful ways so that we can have conscious thought, perceive sensory information, learn and form memories, and have a personality. When we zoom in on this bigger picture of complex neural circuity, we see that a set of neurons connected via synapses lie at the core of each neural circuit. Synapses are tiny gaps where chemical messages are transmitted between neurons to relay information. If one neuron is sufficiently stimulated at this gap, it will generate an electrical signal called an action potential which propagates from the cell body all the way to the end of the neuron. In the case of the sciatic nerve, these neurons can be up to one meter long in the human body!

This communication between neurons is best defined as electrochemical, since both electrical and chemical mechanisms are necessary for synaptic transmission and action potential generation. This electrochemical communication is created by a gradient of electrically charged ions, and it is differences in these ion concentrations which make this system so effective. It takes about 1 millisecond for an action potential to occur, making this an incredibly precise – but nonetheless complex – process. Proteins are involved at every step, mediating the transport of ions and the overall electrochemical gradient of communication within and between neurons. These proteins form ion channels that can be specific for transporting particular ions across the cell membrane. For example, calcium channels have specificity for calcium ions, meaning that they are responsible for determining how high or low the concentration of calcium will be inside versus outside the neuron. Because calcium is involved in physiological processes such as neurotransmission, hormonal secretion, and gene expression, dysfunction in these calcium channels may result in abnormal behavioral phenotypes.

Neuropsychiatric disorders consist of a wide array of symptoms ranging from intellectual disability to depression. Given these vast differences in symptomology, it makes sense that many different biological explanations are possible for a given neuropsychiatric disorder. However, despite the many proposed etiologies, most of these disorders are still not well understood. So,

what is it, exactly, that makes things like bipolar disorder, schizophrenia, and autism spectrum disorder so difficult to study? One of the largest challenges we face in studying these disorders is a concept in psychology called equifinality. Equifinality refers to the idea that multiple different factors can lead to the same disorder: factors like stress, genetic mutations, and socioeconomic status, among others. This adds a significant level of complexity to studying any one disorder, because there is likely to be wide variability from person to person in the way they develop a disorder. Furthermore, differences in the environmental conditions a person is surrounded with is also likely to contribute to variations in the onset of a neuropsychiatric disorder. These differences are difficult to recapitulate in a laboratory setting, but hope is not lost.

Over the past twenty years, genetics research has deepened our understanding of the way in which many disorders may or may not be inherited. It is known that 99.9% of our DNA is identical to one another, but the variability of the other 0.1% makes a huge difference for genetic diseases (Crow, 2002). Genome-wide association studies (GWAS) have been employed to identify specific genetic variations that are highly associated with given diseases. These studies work by analyzing the genome for variations which occur more frequently in people with a certain disease and compares them to people without that disease. Single-nucleotide polymorphisms (SNPs) are one type of genetic variation which have proven to serve an integral role in the genetic explanation for who is more at risk for developing a particular disease. A SNP is the result of a single nucleotide, or genetic building block, being substituted for another nucleotide in a person's genetic code. Each person has approximately three billion nucleotides, so why does a change in just one lead to the potential of developing a serious, sometimes fatal, disease? And moreover, how can we use these identified SNPs to better understand the biology underneath a specific illness?

Most psychiatric disorders are polygenic, meaning that many genes contribute to the onset of one disorder. However, if we are able to identify even just one of the many possible SNPs associated with a certain disorder, we can use that information to learn more about what that specific genetic mutation does to the human body. For example, consider a SNP in a gene which is found to be associated with high risk for developing fragile X syndrome. Upon closer investigation, it is discovered that this particular mutation occurs on a gene that normally codes for a protein called fragile X mental retardation protein (FMRP). This protein is essential for

normal brain development, as it plays a role in how neurons are connected to each other. As a result of this single gene mutation, the individual is not able to make enough FMRP and thus can go on to develop severe intellectual disability, abnormal speech patterns, and even increased anxiety (Myrick et al., 2015). Fragile X syndrome is a prominent example of how a SNP can indicate associated risk for development of a life-altering disease. However, fragile X syndrome is a monogenic disease, meaning the development is attributed to mutations in only one gene. This is a rare scenario, but it highlights the way which the identification of SNPs can help us to study diseases. In addition to multiple genes giving rise to a single disease, the opposite may also occur: pleiotropy is the phenomenon which refers to a single gene producing several phenotypes. As such, studying the biological effects of even one SNP often helps further the understanding of how multiple different diseases function.

To draw the connection between identified SNP and biological consequence, there are several steps that must be taken in the laboratory. First, we must know the genomic region where the SNP is located. At this point, there are two possibilities: the SNP is located in a region of DNA which codes for a specific protein, or the SNP is located in a region of DNA that does not code for a specific protein. The latter case is much more difficult to study, because there is much more variability in the effect this mutation could have on the rest of the genome. If we have a SNP in a DNA region which does code for a known protein (i.e. the first scenario) we can then design an animal model to study how that SNP affects the protein of interest. More specifically, we can develop a model organism in which only that single nucleotide is substituted, then see if there are resulting biological differences between this mutated model compared to a normal organism. This technique of fine-tuned genetic manipulation is called transgenesis, and the individual gene being mutated is called the transgene. If we manipulate a gene in a mouse model to create a transgenic mouse, we can then determine if the mutation results in a change in the protein compared to the normal, non-transgenic, mouse. Once we know how the protein expression levels are affected, the next step is to see how this altered protein level affects cellular processes. Depending on the protein of interest, this could result in severe dysfunction of biochemical mechanisms underlying multiple different diseases.

A recent GWAS found a SNP located near the *CACNA1C* gene to be associated with increased risk for multiple different psychiatric diseases (Smoller et al., 2013). This gene

encodes for part of a protein called $Ca_V1.2$, a subtype of calcium channel which controls the cellular concentration levels of calcium ions involved with a neuron's decision to fire an action potential (Deisseroth et al., 1996). The SNP mutation in this gene has been shown to alter the sensitivity level of $Ca_V1.2$ in a way that may confer abnormally high calcium concentration levels inside the cell (Bhat et al., 2012). A SNP also exists on the *CACNA1D* gene, which codes for another calcium channel called $Ca_V1.3$. Similar to the SNP near the *CACNA1C* gene, the *CACNA1D* mutation is associated with increased risk for developing a neuropsychiatric disorder (Ross et al., 2016a). Mutations in *Cacna1c* and *Cacna1d* have also each been shown to cause memory impairment in mouse models (McKinney and Murphy, 2006a; White et al., 2008). However, the changes in calcium dynamics that result from these heritable genetic mutations have yet to be fully characterized. Due to the demonstrated importance of $Ca_V1.2$ and $Ca_V1.3$ in multiple neural circuits, it is valuable to understand how calcium concentrations are affected by these mutations.

To investigate changes in calcium dynamics, we make use of a technique called *in vitro* calcium imaging. In this method of visualizing calcium activity, a bioluminescent molecule derived from luminescent jellyfish – called *aequorin* – fluoresces green when it comes into contact with a calcium ion (Shimomura et al., 1962). The brighter the green light glows in a given cell, the more calcium present. By comparing calcium dynamics of neurons containing the SNP linked to altered $Ca_V1.2$ or $Ca_V1.3$ functionality to the calcium dynamics of non-mutated neurons, we can develop the understanding of how this mutation might contribute to neuropsychiatric disorders.

Critical Literature Review

Genetic research advancements for neuropsychiatric disorders

Over the past thirty years, substantial progress been made in the field of genetics pertaining to neurological and psychiatric disease states. In 1983, Huntington's disease (HD) became the first mapped human genetic disease (Gusella et al., 1983). To accomplish this, scientists established large family studies and analyzed polymorphic DNA markers linked to HD. As a result, they were able to localize the mutation to chromosome 4. It was not until 1993,

however, that the genetic mutation resulting in HD development was isolated further to chromosome 4p16.3 (MacDonald et al., 1993). Even after defining the genetic locus of HD using positional cloning, *MacDonald et al.* were not able to specify affected biological mechanisms resulting from the mutation in the *HTT* gene. In fact, the role of Huntingtin protein, the product of *HTT* transcription and translation, remains unknown (Moldovean and Chiş, 2020).

The story of HD research is a motivating one, because it resembles the advancements the field has made in elucidating the biological underpinnings for a given disease. Since the discovery of the genetic locus for HD, many diseases have shared a similar narrative – owing their success to high-throughput sequencing and the development of genomic comparison studies. However, it is uncommon that a disease is monogenic like HD. Usually, a given disease phenotype is multifactorial, with multiple mutations located at different regions throughout the genome. Understanding the physiological effects of even one of these mutations allows researchers to more holistically characterize a disorder, with the hope of eventually developing an effective therapeutic treatment. Since the discovery of *HTT* as the first disease gene, genetic tools have become much more advanced in identifying high risk-associated loci.

Rather than relying on a particular family pedigree and linkage analysis to identify a locus for a disease gene, a genome-wide association study (GWAS) uses markers across the genome to investigate association between particular genes and a given phenotype of interest. The first GWAS was published in 2002 (Ozaki et al., 2002), and since then then use of single-nucleotide polymorphisms (SNPs) have advanced the study of genetic mutations that hold high potential for causing a particular disease. As the name suggests, a SNP refers to a point mutation. Often, a SNP will occur within or near a gene, in which case there is increased potential for that mutation to have a direct effect on the biological mechanisms associated with that given gene. An advantage of conducting a GWAS over a linkage analysis it the unbiased nature of a GWAS, since it is essentially hypothesis-free. Because GWA studies screen a population of affected individuals, they have much higher genetic resolution than a pedigree-based linkage analysis. Since a GWAS assumes individuals are not related, a high-risk SNP may be more tightly linked to genetic contribution in disease etiology than in a family linkage study.

For many years, twin concordance studies have suggested that disorders such as autism, schizophrenia, and bipolar disorder are highly heritable (Folstein and Rutter, 1977; McGuffin et

al., 1984, 2003). More recently, GWA studies have shed light on specific heritable mutations associated with increased risk for development of neuropsychiatric disorders. As such, these advancements have given rise to research projects aimed at understanding mechanisms by which genetic mutations may contribute to pathological phenotypes. Once a SNP has been marked as having high association with a certain disorder via GWA studies, subsequent research of that disorder is then able to be conducted with a much finer lens. For this reason, calcium channels have been of increasing interest in the field, as mutations in these proteins have been identified as significant biological underpinnings implicated in many diseases and behavioral abnormalities.

Introduction to calcium channels

Calcium is a fundamental signaling molecule that mediates neurotransmission, hormonal secretion, gene expression, and muscle contraction, among other physiological processes. Without calcium channels, many of these processes would not be possible. As such, disruptions in normal calcium signaling can have severe repercussions in terms of health and well-being.

Calcium channels are a class of ion channels with selective permeability to calcium ions (Ca^{2+}). There are two main superfamilies of calcium channels: ligand-gated calcium channels, and voltage-gated calcium channels (VGCCs). It is important to note that these are not the only ion channels capable of transmitting calcium across the cell membrane, as non-selective cation channels such as transient receptor potential (TRP) channels also play a key role in this process. However, ligand-gated calcium channels and VGCCs function in a Ca^{2+}-specific manner and will thus be the focus of this discussion.

Ligand-gated calcium channels form a group of transmembrane proteins which rely on the detection of a chemical messenger (ligand) to open and allow the passage of Ca^{2+} ions through the cellular membrane. These calcium channels, also known as ionotropic receptors, tend to localize on or around the postsynaptic neuronal membrane. Here, neurochemical messenger molecules (neurotransmitters) bind to these receptor channels and cause a conformational change. This structural change opens the channel for Ca^{2+} ions to pass through, effectively transmitting information from the presynaptic terminal to the postsynaptic neuron. Drugs used to suppress the cough reflex, such as dextromethorphan, target a type of ligand-gated ion channel called *N*-methyl-*D*-aspartate (NMDA) receptors, which are permeable to not only

Ca^{2+} but also sodium (Na^{+}) and potassium (K^{+}) ions (Ascher and Nowak, 1987). Non-competitive receptor antagonists like dextromethorphan work by binding to an allosteric site on these ligand-gated channels to prevent receptor activation. Pharmacological interventions like this are useful in the treatments of many medical ailments, as they capitalize on the comprehension that investigative research has provided about these ligand-gated ion channels.

While ligand-gated ion channels are important components of normal cell function, VGCCs are directly involved in transducing membrane potential changes to make cellular communication possible. The imperative nature of VGCCs in neurotransmission makes for a very interesting field of study, as mutations which confer functional changes in these channels may have dramatic, sometimes lethal (Rosati et al., 2011), consequences.

Voltage-gated calcium channels (VGCCs)

The action potential is the fundamental unit of communication in the nervous system. To make this mechanism of communication function seamlessly, VGCCs are integrated in the plasma membrane and are able to detect depolarizing changes in membrane potential. They are responsible for mediating the 20,000-fold gradient of calcium concentration in response to membrane depolarization (Clapham, 2007). Directly after an action potential fires, calcium rushes into the cell through VGCCs and facilitates the release of neurotransmitter from the presynaptic bouton.

Although there are five different types of VGCCs, there are a total of ten different proteins in the umbrella of the VGCC family – each with slightly different electrophysiological properties. To better understand the differences between individual channels, it is important to first address the structural composition that makes up the framework of a VGCC protein.

Depending on the particular VGCC, the protein is composed of 4 or 5 subunits: α_1, $\alpha_2\delta$ (α_2 and δ), β, and γ (Bekircan-Kurt et al., 2015). The pore-forming subunit, also called the principal channel protein α_1, is the defining feature of VGCCs in the current nomenclature. Specifically, there are ten different genes known to encode unique variations in the α_1 subunit (Catterall, 2011) – and thus there are ten different kinds of VGCCs. Each of these ten variations in the α_1 subunit varies in current properties and pharmacology (Catterall, 2011). The α_1 subunit is 190 kDa in size and 2000 amino acid residues long (Tanabe et al., 1987), and this whole structure constitutes the ion channel pore which mediates Ca^{2+} flux. More than this, the pore-

forming subunit also contains voltage-sensitive domains to detect shifts in membrane potential. After sensing a depolarizing voltage change large enough to induce VGCC opening, it selectively allows Ca^{2+} to pass through due to its selectivity filter and activation gate. Other domains exist within the α_1 subunit which are responsible for driving protein-protein interactions or are the sites of modulatory activity. Due to the many qualities exhibited by the α_1 subunit, it is interesting to note that expression of an α_1 subunit alone in a heterologous cell is sufficient to recapitulate a functional ion channel – though with altered physiological properties from normally-functioning VGCCs (Campiglio and Flucher, 2015). This principal channel protein consists of four homologous repeats of six transmembrane domains, and is the central component of a VGCC which attaches to the other subunits of the protein complex (Catterall, 2011).

While the α_1 subunit is the defining characteristic of a VGCC, the other 4 auxiliary subunits must be taken into consideration. The calcium channel β subunit is the cytoplasmic protein in the VGCC complex, and has been shown to be involved with regulating voltage sensitivity and activation/inactivation kinetics of VGCCs (Neely et al., 1993; Josephson and Varadi, 1996). The $\alpha_2\delta$ auxiliary subunit is made of a disulfide-bridged dimer of the α_2 and δ protein subunits (Takahashi et al., 1987). This subunit makes up the extracellular domain of the ion channel, and has a main function of increasing Ca^{2+} current (though also implicated in biophysical protein modifications) (Davies et al., 2006). Both the β and $\alpha_2\delta$ auxiliary subunits play an important part in ensuring proper channel folding and overall protein trafficking (Dolphin, 2016). Lastly, the γ_1 subunit is an integral membrane protein found only in VGCCs in skeletal muscles (Dolphin, 2016).

As previously stated, the ten different VGCCs are characterized by the specific pore-forming (α_1) subunit integrated into the protein complex. The calcium current of a given VGCC recorded at voltage of activation, as well as inactivation kinetics and pharmacological properties, were used to split the ten VGCCs into five types: L, P/Q, N, R, and T. The letters designated to each VGCC signifies an attribute of the observed calcium current for that channel: “L-type” refers to large calcium currents; “P/Q-type” refers to the discovery of calcium currents in Purkinje neurons (Llinás et al., 1989); “N-type” refers to a calcium current somewhere in between L- and T-type currents; “R-type” refers to the apparent resistance these channels had to pharmacological blockers of L-, P/Q-, and N-type calcium currents (Randall and Tsien, 1995); and “T-type” refers to transient calcium currents. In conjunction with the calcium current

classifier, the specific α_1 subunit is also appended to the end of the indicated VGCC gene name (e.g. L-type VGCCs *CACNA1C* and *CACNA1D* have an α_{1C} and α_{1D} pore-forming subunit, respectively). Due to the somewhat convoluted nature of this nomenclature, a secondary mechanism of naming has been adopted by the field – though the original naming system also remains in use. In this new classification system, the protein is identified with "Ca" to symbolize its permeability to the Ca^{2+} ion, and a "V" is used in the subscript (Ca_V) to indicate that these ion channels are voltage gated. This designation is then followed by a numerical representation of the α_1 subunit based on homological amino acid sequence (Ca_V1, Ca_V2, and Ca_V3) to indicate the family. Lastly, the order in which the ion channel of each family was discovered is appended to the numerical family representation (e.g. $Ca_V1.1$, $Ca_V1.2$, $Ca_V1.3$, and $Ca_V1.4$) (Ertel et al., 2000).

Voltage-gated calcium channels are located throughout the entire body and are well-known by many for their role in neurotransmitter release from presynaptic neuron terminals in response to depolarizing membrane potential changes. However, in referring to these physiological properties, it is important to clarify that not all VGCCs are localized to presynaptic boutons and participate in neurotransmitter release. In fact, the Ca_V2 family are the VGCCs most associated with this aspect of neurotransmission – with the Ca_V3 family also being involved in presynaptic neurotransmitter release in some synapses (Cao and Tsien, 2010; Carbone et al., 2014). The L-type VGCCs (LVGCCs) differ from their P/Q-, N-, R-, and T-type counterparts in that they do not play a role in the release of neurotransmitters from the presynaptic neuron (Biase et al., 2008; Jenkins et al., 2010).

L-type voltage-gated calcium channels (LVGCCs)

L-type voltage-gated calcium channels (LVGCCs) make up the Ca_V1 family of VGCCs, and are located throughout the body (Catterall, 2011). These four ion channels are expressed at different levels depending on the region of the body, but $Ca_V1.2$ and $Ca_V1.3$ are the only LVGCCs with high expression in the brain (Hetzenauer et al., 2006). On the other hand, $Ca_V1.1$ and $Ca_V1.4$ are more abundantly expressed in skeletal muscle and the retina (Striessnig et al., 2010). Typically LVGCCs are localized to the neuronal cell soma and dendrites in the mammalian nervous system (Hell et al., 1993), but a gap in the current literature exists regarding how these expression patterns may be affected in neuronal cultures. With the goal of elucidating

differences in gene expression in culture versus *in vivo*, a study in 2008 performed a series of comparative microarray experiments between retina explants *in vitro* and *in vivo* (Liu et al., 2008). Remarkably, about 75% of the expressed genes had equivalent expression volume *in vivo* as *in vitro* – and only 1% of the expressed genes were reported to show a change threefold or greater (Liu et al., 2008). Though this study was conducted using mouse retina explants, the need for characterizing *in vitro* models of *in vivo* mechanisms is important to consider. If up to 6% of the gene population underwent even modest expression level changes in culture as compared to *in vivo* models (Liu et al., 2008), this means that there is potential for similar *in vitro* artifacts of gene expression in other contexts as well. Furthermore, the idea that gene expression can change due to variability in environmental conditions likely transcends retinal explant models; it may also be true that LVGCC models experience these changes as well.

Importantly, recent *in vitro* findings suggest that LVGCCs have a similar somatodendritic Ca^{2+}signal and molecular architecture as reported in brain neurons (Vierra et al., 2019). This study used both hippocampal neuron cultures and hippocampal slices, because the distribution of LVGCC expression and localization in hippocampi has been previously well-described (Hell et al., 1993). Although the discovery that LVGCCs have a similar molecular and physiological functionality in culture as in neurons of the intact brain, this study did not holistically address potential gene expression alterations using microarray comparisons like *Liu et al.* Instead, the researchers only performed immunostaining: a useful method of determining expression localization, but not the best way of determining expression levels. It should also be noted that these findings have yet to be recapitulated. The distinction between *in vitro* and *in vivo* experiments is important, because results of these studies may have different implications depending on the question being addressed. For example, when studying the differences in physiological properties of LVGCCs due to genetic mutations associated with an abnormal phenotype, it must be confirmed that the model being used is truly representative of the biological pathology and not just an artifact of the environmental conditions.

As was stated earlier, the expression of LVGCCs, namely $Ca_V1.2$ and $Ca_V1.3$, have been well characterized in the hippocampus. While $Ca_V1.3$ has a more general expression pattern, the expression of $Ca_V1.2$ is more restricted. In hippocampal CA1 there is high expression of $Ca_V1.2$ in cell bodies of the pyramidal layer. Additionally, $Ca_V1.2$ is expressed in the cell bodies and dendrites of hippocampal CA2 and CA3, and the dendritic arborization of the dentate gyrus. In

contrast, $Ca_V1.3$ localizes to cell bodies and dendrites throughout the entire hippocampus (Hell et al., 1993). One other difference between $Ca_V1.2$ and $Ca_V1.3$ is their voltage sensitivity: $Ca_V1.2$ channels begin opening at about -40 mV, while $Ca_V1.3$ channels begin opening at about -60 mV (Helton et al., 2005).

Learning and memory: the role of LVGCCs

The hippocampus is the memory subunit of the brain, and is a primary region of adult neurogenesis – a process with demonstrated importance for memory encoding (Altman, 1963; Toda et al., 2019). Given the high expression of LVGCCs in the hippocampus, and LVGCC's involvement with adult neurogenesis (Temme et al., 2016), it is unsurprising that these ion channels have themselves been shown to mediate memory consolidation (McKinney and Murphy, 2006).

At present, the field commonly uses genetically manipulated mouse models to study the role of LVGCCs, specifically $Ca_V1.2$ and $Ca_V1.3$, in memory encoding. To accomplish this, mouse models have been generated with each aspect of LVGCC expression manipulation in the hippocampus: $Ca_V1.2$ over-expression ($Ca_V1.2$-HA), $Ca_V1.2$ deletion ($Ca_V1.2$-KO), $Ca_V1.3$ over-expression ($Ca_V1.3$-HA), and $Ca_V1.3$ deletion ($Ca_V1.3$-KO) (Platzer et al., 2000; White et al., 2008; Krueger et al., 2017). By only altering the expression of a LVGCC, we can further define the physiological function of a single ion channel. Thus, these genetic alterations are powerful tools and have allowed for significant advancements elucidating the role $Ca_V1.2$ and $Ca_V1.3$ play in important biological processes.

Importantly, modifications to postburst afterhyperpolarization (AHP) kinetics accompanies memory encoding (Moyer et al., 1996). An AHP consists of a hyperpolarization in the neuronal membrane potential immediately following a burst of spikes. The function of an AHP is to reduce firing by maintaining the membrane potential below spike threshold (Alger and Nicoll, 1980). Reducing the AHP results in a direct increase in neuronal excitability allowing for possible increases in firing rate from glutamatergic hippocampal neurons. The precise timing of this postsynaptic excitability window is thought to be significant for memory consolidation (Moyer et al., 1996), and as such is of high interest in the field of learning and memory research.

In the scientific lexicon surrounding AHPs, it is common to subdivide them into three components: slow (s), medium (m), and fast (f) AHPs. The efflux of K^+ ions at the end of an

action potential is the cause of each of these AHPs, with the principal difference between the three being the temporal scale of repolarization (as indicated by the terms "slow," "medium," and "fast"). The fAHP lasts about 1-5 ms and is dependent on both calcium concentration and voltage (Lancaster and Nicoll, 1987). The mAHP has a decay constant of about 100-200 ms, and the sAHP has a decay constant on the order of 1000-5000 ms (Storm, 1990). The fAHP operates through BK-type channels (Storm, 1987), but the channels responsible for the K^+ current underscoring mAHPs and sAHPs remains unclear. The concentrations of calcium necessary for the K^+ responsible for these AHPs is also unknown.

A link exists between varying sAHP magnitude and memory consolidation during learning performance tasks. A reduced sAHP was observed in successfully trained mice in comparison to untrained mice performing the same learning task (Disterhoft et al., 1996). The dynamic of sAHP magnitude is intricate: too high and neurons will be overly inhibited, too low and neurons will be overly active. In fact, increased sAHPs, and thus longer refractory windows, are linked with decreased performance in learning tasks (Murphy et al., 2004, 2006). Likewise, sAHPs of smaller magnitude resulted in impaired memory performance (Perkowski and Murphy, 2011).

In 2006, *McKinney and Murphy* conducted an experiment using $Ca_V1.3$-KO mice to study neural mechanisms of memory. This was the first study that justifiably concluded that $Ca_V1.3$ mediates memory consolidation, as indicated by $Ca_V1.3$-KO mice displaying impaired contextual fear conditioning but normal freezing patterns when compared to wild-type littermates (McKinney and Murphy, 2006). Because decreased sAHPs could result in memory impairment (Perkowski and Murphy, 2011), and the deletion of $Ca_V1.3$ (but not $Ca_V1.2$) results in decreased sAHP amplitude (Gamelli et al., 2011), the findings of this 2006 study are robustly accepted in the field. Of note, the Murphy Lab group has also shown that $Ca_V1.2$ is involved with memory encoding – as conditional knockout ($Ca_V1.2$-KO) mice displayed impaired spatial memory performance in comparison to wild-type littermates (White et al., 2008).

Taken together, there is substantial evidence suggesting that a loss of function mutation in $Ca_V1.2$ or $Ca_V1.3$ results in impaired memory performance. However, the physiological role of calcium underpinning these abnormal phenotypes remains elusive. To fully comprehend the mechanisms of action by which these LVGCCs operate it is imperative that we design experiments that allow us to begin drawing conclusions about the calcium dynamics resulting

from altered LVGCC expression levels. Although learning and memory processes have been shown to be affected by LVGCC deletions, understanding the physiological implications of these calcium channels will open the door for research in a context even broader than that of the hippocampus.

Neuropsychiatric disorders: mutations in LVGCCs

L-type voltage-gated calcium channels mediate postsynaptic responses within pathophysiologically relevant neural pathways associated with numerous neurodevelopmental and psychiatric disorders (Deisseroth et al., 1998; Mermelstein et al., 2000). Of these pathways, both $Ca_V1.2$ and $Ca_V1.3$ are functionally important in the hippocampus, amygdala, and mesolimbic reward system (Rajadhyaksha and Kosofsky, 2005; McKinney and Murphy, 2006; Temme and Murphy, 2017): all of which are brain regions responsible for mediating behavior patterns. Given this, it is reasonable to consider the possibility that even slight deviations from the normal transcript may result in altered brain function.

There exists a SNP near *CACNA1C*, the gene which encodes the α_{1C} subunit of $Ca_V1.2$, which has been linked to significant risk for development of Timothy syndrome – a syndromic autism spectrum disorder caused by a gain-of-function missense mutation. In the time since the association of this gene with high risk for developing Timothy syndrome was published in 2004 (Splawski et al., 2004), significant developments have been made in attempt to uncover how this mutation contributes to the autistic phenotype (Boczek et al., 2015). While this missense mutation has been shown to significantly reduce voltage-sensitivity of $Ca_V1.2$ (Splawski et al., 2004), there is a need to understand the resulting effects on calcium dynamics.

In 2008, a different SNP located near *CACNA1C* was identified as one of the strongest susceptibility loci for bipolar disorder (Ferreira et al., 2008a). Subsequent studies have elucidated the role of the *CACNA1C* risk allele, showing its responsibility for upregulated expression levels of $Ca_V1.2$ (Bhat et al., 2012). While bipolar disorder is a psychiatric disorder specifically referenced in these GWA studies, other research has found alterations in the expression of $Ca_V1.2$ to yield behavior representative of schizophrenia (Bigos et al., 2010).
More recently, in 2016, the association of a *CACNA1D* mutation with bipolar disorder has also been implicated (Ross et al., 2016). Alterations in this gene would directly affect $Ca_V1.3$ function, as it is the gene which encodes the α_{1D} pore-forming subunit of the LVGCC.

The demonstrated importance of genetic mutations affecting the principal channel protein cannot be ignored. To clarify the contribution these genetic mutations may have on the aforementioned behavioral and physiological phenotypes, genetically manipulated mouse models may be used to study underlying calcium dynamics. Specifically, an over-expressed $Ca_V1.2$ model would serve to recapitulate the gain-of-function mutation associated with neuropsychiatric disorders. Additionally, an over-expressed and knockout $Ca_V1.3$ model would be helpful to study, as it is not known if the effect of disorder-associated SNPs located near *CACNA1D* confers a gain- or loss-of-function mechanism of action.

Specific Aims

The goal of this study was two-fold. First, *in vitro* calcium imaging was utilized to further understand how calcium dynamics are affected due to alterations in *Cacna1c* or *Cacna1d* expression levels. These results provide novel insight into how gain- or loss-of-function mutations in LVGCCs contribute to pathophysiological phenotypes (McKinney and Murphy, 2006; Bhat et al., 2012). A second initiative of this study was to localize expression of $Ca_V1.2$ and $Ca_V1.3$ in culture, as these *in vitro* expression patterns have not been well-described in current literature. Further defining where these LVGCCs are localized *in vitro* is helpful for narrowing our focus to specific cell regions, yielding higher spatial resolution for future calcium imaging experiments. Together, these studies work cohesively to elucidate the location and the mechanism by which genetic mutations responsible for modified LVGCC expression levels contribute to altered calcium dynamics.

Materials and Methods

Mice

Except where noted, all genetically engineered mice were bred in house and wild-type littermates were used as controls. All mice used in this study were generated or maintained (>20 generations) on a C57B/L6Tac genetic background. Experiments included four different mouse models: mice that over-expressed $Ca_V1.2$ or $Ca_V1.3$, and mouse models which completely lacked expression of $Ca_V1.2$ or $Ca_V1.3$ (so called "knock out" [KO] mice).

In both over-expression models, full length transcripts for the pore-forming subunit were modified to contain a hemagglutinin (HA) epitope tag in an extracellular loop and are referred to here after as the $Ca_V1.2$-HA and $Ca_V1.3$-HA lines. The over-expression of $Ca_V1.2$ was driven by the ubiquitous CAG (CMV enhancer, chicken beta-actin) promoter whose activity is regulated by a lox-P flanked stop codon cassette located 5' to the ATG sequence of the transgene. For the current study, the $Ca_V1.2$-HA mice were crossed with mice in which expression of Cre Recombinase was driven by the Synapsin 1 promoter ("Synapsin-Cre" mice; Zhu et al., 2001) which restricted $Ca_V1.2$-HA expression to neurons. Expression in the $Ca_V1.3$-HA line was driven by the alpha calcium calmodulin kinase II promoter and is thus restricted to glutamatergic neurons in the forebrain (Krueger et al., 2017).

Mice lacking $Ca_V1.2$ (referred to here after as $Ca_V1.2$-KO mice) were engineered such that $Ca_V1.2$ could be deleted in a cell-type specific manner because the global $Ca_V1.2$-KO mice exhibit embryonic lethality (presumably due to expression on the heart). To achieve conditional deletion, mice in which the second exon of *Cacna1c* (the gene encoding $Ca_V1.2$) was flanked by lox-P sites (White et al., 2008) were crossed the Synapsin-Cre mice, resulting in apportion of the offspring which were $Ca_V1.2^{f/-}$:Cre^{+}. These mice were intercrossed to obtain pure wild-type mice ($Ca_V1.2^{f/f}$:Cre^{-}) and true $Ca_V1.2$-KO mice ($Ca_V1.2^{-/-}$:Cre^{+}).

Mice lacking $Ca_V1.3$ (referred to here after as $Ca_V1.3$-KO mice) were made by homologous recombination such that exon 2 of *Cacna1d* (the gene encoding $Ca_V1.3$) was replaced by a neomycin-resistant cassette which results in a missense frame shift effectively producing a heterozygous null mutation. Heterozygous null $Ca_V1.3$ mice were intercrossed to obtain $Ca_V1.3$-KO mice and wild-type littermates.

All mice were fed *ad libitum* and kept on a 14:10-h light:dark schedule. All procedures involving mice were approved by the University of Michigan Institutional Animal Care and Use Committee (approval number for the protocol: PRO00008648; principal investigator: Geoffrey Murphy, PhD) and performed according to the National Institute of Health guidelines for animal care.

Hippocampal neuron cultures

To prepare cell cultures, hippocampi were harvested from mouse pups at postnatal day 1-2 following genotyping. Meninges were removed to facilitate tissue extraction. This was done in HEPES buffered saline solution (HBSS) – a physiological saline containing the following (in mM): NaCl 136, KCl 2.5, HEPES 10, glucose 10, $CaCl_2$ 2, and $MgCl_2$ 1.3. The HBSS was then adjusted to pH 7.4. The hippocampi were isolated and harvested, then placed in HBSS on ice. An 18 mm glass coverslip was placed in a 35 mL dish. A poly-D-lysine agent from the freezer was added to the coverslip to supply negative charge, allowing negatively-charged lipids from cell membranes to adhere well. In 2 × 10 mL HBSS vials with 10 mM hepes, the following 2 ingredients were added: L-cysteine (3.2 mg) and L-papain (240 μL). L-cysteine activated L-papain to enhance its enzymatic activity, so that it was able to break down protein bonds between synapses. Vials were sterilized with ethanol and placed in a 37°C water bath to facilitate mixture.

HBSS solution was removed from hippocampal slice vials, and the L-papain solution was introduced through a filter into the vials. These vials were placed back in the water bath at 37°C for 15 min. The tubes were inverted every 2.5 min to ensure that the solution was equally distributed. After 15 min, the hippocampus was washed 3 times with cold HBSS, then the vial was placed on ice. All HBSS solution was removed from the hippocampal vials and placed in new vials; care was taken to not remove the hippocampal slices. The new vials were centrifuged for 5 min at 0.6 relative centrifugal force (RCF) to allow cells to aggregate into a pellet at the bottom of the tube. This allowed us to get rid of HBSS solution and replace with NbActiv4 (BrainBits, Nb4) for culture. Nb4 is the salt solution the neurons are cultured in: it has factors that mimic developmental physiological conditions (with Ca^{2+}, Mg^{2+}, cholesterol, B27, glutamic acid, and estrogen with added glucose). After centrifuge, HBSS solution was removed, and the

pellets were placed in 50 µl of NB4 for 1 hour. After 1 hour, 2 ml of Nb4 were placed on plates, and moved to a humidified incubator at 95:5 (O_2: CO_2) and 37ºC.

Antibodies

The antibodies used included the following: anti-HA (Roche; rat, #11867423001, immunocytochemistry [ICC] 1:500), anti-MAP2 (abcam; chicken, #ab5392, ICC 1:5000), goat anti-rat secondary (abcam; #ab150167, ICC 1:500, Alexa Fluor 647), and goat anti-chicken secondary (abcam; #ab150170, 1:500, Alexa Fluor 555). Immunocytochemical mounts were treated with ProLong Diamond Antifade containing 4'6-diamidino-2-phenylindole (DAPI; Invitrogen, # P36935).

Immunolabeling of cells

Neuronal cultures were fixed and processed for immunocytochemistry as described by Glynn and McAllister (2006), with the exception that bovine serum was substituted for goat serum. Briefly, primary antibodies were added at given dilutions in 3% goat serum for 1 h followed by washes (3% goat serum in PBS, 5 × 5 min), and secondary antibodies (diluted in PBS) were added for 45 min followed by 5 × 5 min washes in PBS. Confocal images were acquired using an Olympus FV1000 microscope equipped with a photomultiplier tube and a 40× NA objective lens. To obtain these images, we used Olympus Fluoview software and lasers with the following wavelengths (in nm): 405, 561, 633. This excitation resulted in the following respective photon emission wavelengths (in nm): 421, 565, 647.

Confocal fluorescence images were analyzed for colocalization using the JACoP plugin for Fiji (Bolte and Cordelières, 2006). The Pearson R correlation coefficient was created using spatially matched pixels for two images of different fluorescent intensities (Costes et al., 2004). Automatic thresholding and a Costes randomization of N = 20 was applied. Images presented in this study were subjected to rolling ball background subtraction and Gaussian Blur of Sigma (radius) = 0.5.

In vitro calcium imaging

In vitro calcium imaging was employed to functionally assay voltage-gated calcium channel activity of genetically manipulated mouse models. Calcium imaging was used as a surrogate for traditional electrophysiology to observe differences in patterns of action potential firing, because this technique allows observation of multiple neurons simultaneously, yielding a higher throughput than electrophysiological studies. Additionally, *in vitro* calcium imaging allows for a better temporal analysis than electrophysiology when distinguishing between individual cell bodies and dendrites.

Imaging was conducted after 14–21 days *in vitro* (DIV), with the cells being fed every 3-4 days. A 3-day window without feeding was maintained between the most recent change in media and the first day of imaging. Spontaneous and evoked Ca^{2+} transients of neurons cultured under control conditions were compared. Cell cultures were loaded with calcium dye Fluo-5 AM (Invitrogen) in a 1:1000 HBSS dilution and incubated for 10 min. The dye solution was then aspirated, and the cell cultures were washed twice for 1 min with HBSS before transferring the cover slip to the microscope stage for recording. Once the mounted on the stage, 100 µL HBSS was added on top of the coverslip.

For each dish, imaging was conducted under two conditions: spontaneous activity and 20 Hz stimulation. For recording evoked stimulation, there was an event delay of 40 seconds followed by a 50-100 V stimulation. To enumerate, the 20 Hz stimulation occurred for 2 seconds, 40 seconds into the recording time, totaling in a 40-pulse stimulation. Each recording lasted for 70-90 seconds to ensure calcium activity returned to baseline post-stimulation at 40 seconds. To capture frames as fast as possible, roughly 130-160 millisecond intervals were used and roughly 530-564 cycles were obtained.

To isolate responses to field stimulation, we blocked synaptic transmission with glutamate receptor antagonists: 10-25 µM CNQX (Tocris) and 50 µM L-AP5 (Tocris) in 100 µL HBSS. This 100 µL blocker solution was added to the 100 µL HBSS already present in the recording chamber. Blockers were added after recording spontaneous activity, and 2-5 min incubation time was allowed before recording activity from evoked stimulation.

The Olympus - IX83 microscope was used together with the Olympus cellSens software to obtain images. Images were acquired using a 20× NA objective lens. Illumination was achieved using a Lumencor SpectraX high intensity LED light engine and images were captured with a Prime 95B QE Backside illuminated high speed CMOS camera (Photometrics). Images were recorded at a capture rate of 0.16 Hz for 90 s, yielding a total of 563 frames per recording. The GFP fluorescent laser (excitation 488 nm) was used to excite photons (emission 509 nm) from the Fluo-5 AM dye loaded into the neuronal cultures. A field of view (FOV) for recording was selected primarily based on density of neurons and glia, along with intensity of calcium indicator dye at baseline. High-intensity neurons were avoided when searching for a FOV, as this indicated potential calcium dye overloading and/or cell death – neither of which is ideal for monitoring calcium activity in this study (**Fig. 1**).

Calcium imaging data was analyzed off line using FIJI (Bolte and Cordelières, 2006). Image stacks were corrected for photobleaching with an exponential fit. A threshold was then applied to create a binary mask image using the DiffImage1C plugin for evoked responses or the dFoverFmovie plugin for spontaneous activity. Next, 10-150 regions of interest (ROIs) were generated using the particle analysis plugin. Both cell bodies and dendrites were considered when selecting ROIs for this study unless otherwise specified. Using the Time Series Analyzer V3 plugin (Balaji, 2014), ROIs were individually analyzed in each frame for changes in fluorescence as indicated by the Fluo-5 AM calcium dye intensity. Graphpad Prism 8 was then used to combine data for visualization and statistical comparison.

Statistical analysis

Graphpad Prism 8 was used to combine data for visualization and statistical comparison. Maximum amplitudes were compared between genotype groups using an unpaired two-tailed *t*-test. An unpaired two-tailed *t*-test was also used to compare Pearson's correlation coefficient (PCC) data when looking for colocalization between MAP2 and HA in immunocytochemistry. These tests were appropriate, because the data were normally distributed and satisfied parametric assumptions. A threshold of α=0.05 was used to determine significance. Sample means and variances are presented as mean $\pm$ standard error of the mean (SEM) throughout this study.

Figure 1

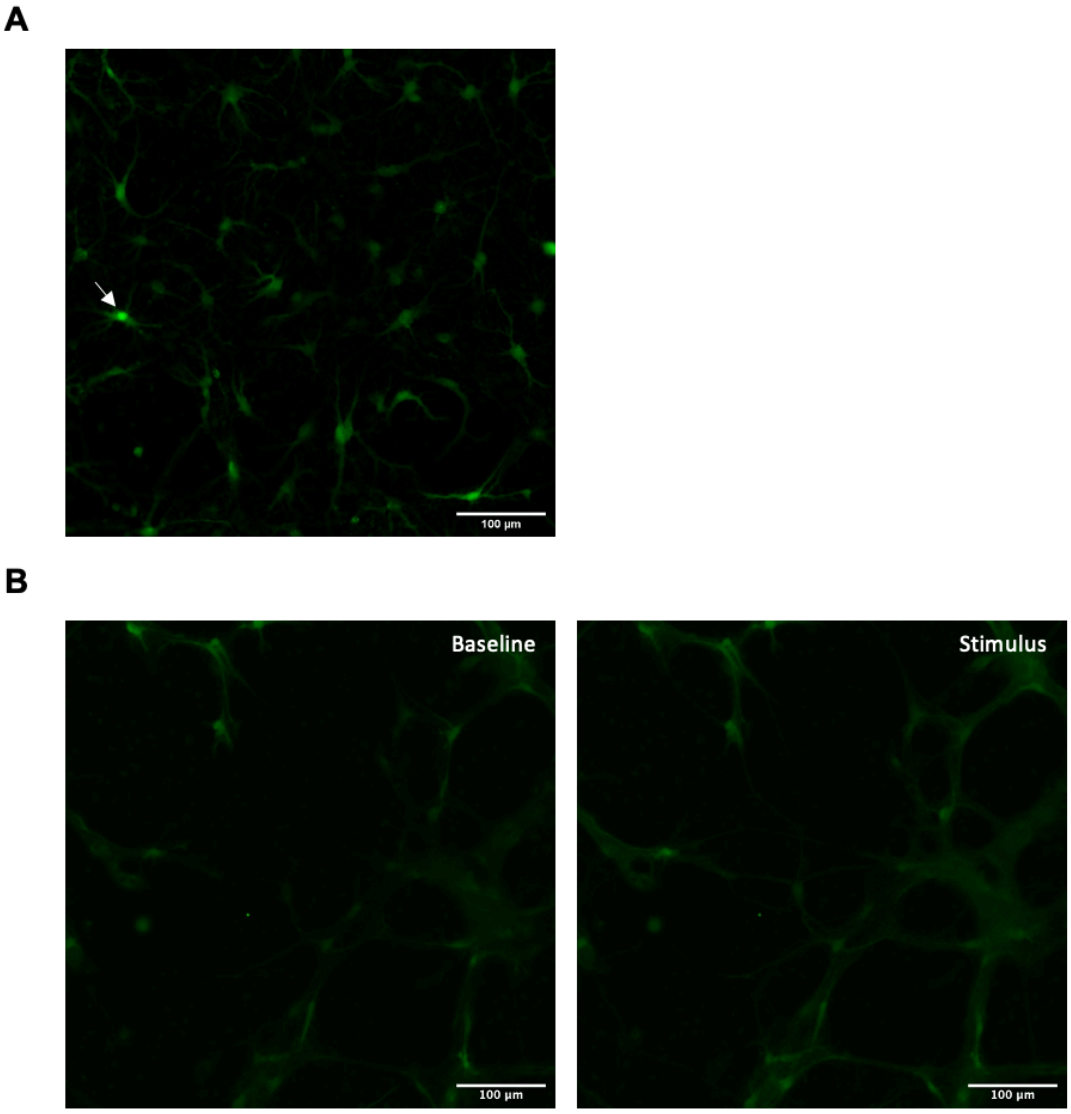

Figure 1. Representative fields of view (FOVs) during calcium imaging. All images in this figure were taken at 20× magnification. **A**, there is relatively high neuron density in this FOV, with a low amount of glia present. The white arrow at left indicates a high-intensity neuron, likely due to calcium dye overloading and/or cell death. Neurons that look like this were avoided if possible. This image was subjected to rolling ball background subtraction and Gaussian Blur of Sigma (radius) = 0.5. **B**, the FOV at left represents baseline fluorescence for a WT neuronal culture, while the right image represents the same FOV in response to a 20 Hz (40-pulse) stimulation at 100 V. These images were corrected for photobleaching using an exponential fit model, with otherwise no image processing.

Results

Initial insight into altered $Ca_V1.2$ and $Ca_V1.3$ calcium dynamics

Previous studies have demonstrated the importance of altered $Ca_V1.2$ and $Ca_V1.3$ expression levels in memory consolidation and neuropsychiatric disorders (McKinney and Murphy, 2006; Bhat et al., 2012). To expand upon these findings, we sought to characterize the calcium dynamics resulting from genetic manipulations of *Cacna1c* and *Cacna1d*. To accomplish this, *in vitro* calcium imaging of mouse hippocampal neuron cultures was employed. Glutamatergic ion channel blockers CNQX and AP5 were applied to eliminate activity due to synaptic activation, and a 20 Hz stimulus of 50 V was introduced 40 seconds into the recording. Calcium activity within neuronal cultures was measured as a function of fluorescent intensity over time, then compared between a genetically manipulated mouse model and a wild-type littermate.

There appeared to be a decrease in calcium transients upon over-expression of $Ca_V1.3$ ($Ca_V1.3$-HA), and an increase in activity due to $Ca_V1.3$ deletion ($Ca_V1.3$-KO; **Fig. 2A**). This is represented by a comparison of average maximum amplitudes of neurons observed within these traces ($Ca_V1.3$-WT=0.2997, $Ca_V1.3$-HA=0.1589; $Ca_V1.3$-WT=0.0808, $Ca_V1.3$-KO=0.2430). Likewise, $Ca_V1.2$-KO neuron cultures appeared to yield increased levels of calcium activity compared to cultures prepared from their wild-type littermates ($Ca_V1.2$-WT=0.1653, $Ca_V1.2$-KO=0.1813; **Fig. 2B**). At the time this experiment was conducted, the $Ca_V1.2$-HA transgenic line had not yet been generated for study and thus are not shown in these graphs. It should be noted that the sample size (N) in this experiment is represented as individual neuronal cell bodies. This is important to address because subsequent experiments presented in this study define N as including both cell bodies and dendrites.

We reasonably expected that over-expression of LVGCCs would lead to an increase in the observed level of calcium activity, and analogously that deletion of these channels would yield a reduction. Although no statistical comparisons were performed, these data provided the first glimpse into a potentially counterintuitive mechanism of action for these LVGCCs. In addition to the seemingly reciprocal pattern of these findings, there were inconsistencies in the level of calcium activity observed in the wild-type control neuron cultures ($Ca_V1.3$-WT=0.2997, 0.0808; $Ca_V1.2$-WT=0.1653). To uncover any truth behind these counterintuitive findings and

account for potential variability between cultures, we next decided to increase our sample size and consider the effects of over-expressing $Ca_V1.2$ on calcium activity in neuron cultures.

Figure 2

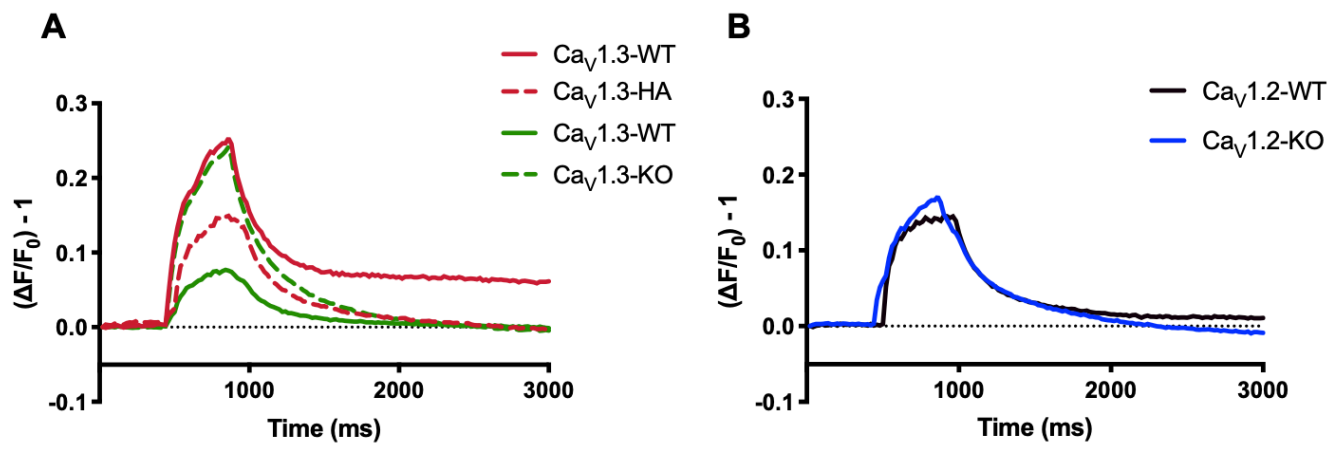

Figure 2. Time traces from a preliminary study conducted in 2017. Time traces displayed here represent average cell body response of a given genotype to a 20 Hz (40-pulse) 100 V stimulus introduced at an event delay of 40 s. In the graphs shown, the 3000 ms surrounding the cellular response to the 20 Hz stimulus is shown. Calcium activity is measured as $(\Delta F/F_0)$-1. **A,** time traces of $Ca_V1.3$-HA neuronal cultures (red dashed) and $Ca_V1.3$-KO neuronal cultures (green dashed) compared to their wild-type (WT) littermates (dark red and dark green, respectively). Data include the following sample sizes: $Ca_V1.3$-HA, N=22, $Ca_V1.3$-WT ($Ca_V1.3$-HA littermates), N=10, $Ca_V1.3$-KO, N=26, $Ca_V1.3$-WT ($Ca_V1.3$-KO littermates), N=8. **B**, time traces of $Ca_V1.2$-KO neuronal cultures (blue) compared to their WT littermates (black). Data include sample sizes: $Ca_V1.2$-KO, N=24, $Ca_V1.2$-WT ($Ca_V1.2$-KO littermates), n=17.

Reciprocal pattern of calcium transients due to manipulated $Ca_V1.3$ expression

Given the inverse relationship of calcium activity observed in our preliminary experiment (**Fig. 2**), we next asked if increasing the sample size of $Ca_V1.3$-HA, $Ca_V1.3$-KO, and $Ca_V1.3$-WT would yield significance. As mentioned previously, $Ca_V1.3$ channels are expressed in both cell bodies and dendrites of hippocampal neurons of the intact brain (Hell et al., 1993). Thus, we decided to consider cell bodies and dendrites together in our analysis of calcium transients (as opposed to only considering individual neuronal cell bodies as ROIs – the method of Figure 2 experiments).

After imaging *in vitro* calcium activity of $Ca_V1.3$-HA neuronal cultures, representative traces of calcium activity were plotted as a function of fluorescent intensity over time (**Fig. 3A**). Upon introduction of a 20 Hz stimulus 40 seconds into recording, calcium transients elicited peak fluorescent amplitude in each time trace. Off-line analysis revealed no significant difference in average maximum amplitude between mutants and $Ca_V1.3$-WT ($p>0.05$; **Fig. 3B**). This lack of significance is likely due to the consideration of entire fields of view as individual samples. Also consistent with our 2017 preliminary experiment, $Ca_V1.3$-KO neuronal cultures appeared to exhibit a decrease in maximum amplitude when compared to wild-type littermates (**Fig. 3D**). However, statistical analysis conferred no significant findings in this comparison ($p>0.05$). There was an error in maintaining a constant image acquisition rate between $Ca_V1.3$-HA and $Ca_V1.3$-KO experiments, so $Ca_V1.3$-KO time traces are plotted as a function of frames rather than time (**Fig. 3C**).

Due to the consistent pattern observed between this experiment and the experiment conducted in 2017 (**Fig 2A**), we expect that increasing the sample size even further in future studies – thus increasing statistical power – would reveal a significant decrease in maximum calcium activity amplitude of $Ca_V1.3$-HA compared to wild-type littermates. Similarly, we would expect increasing sample size in future studies to demonstrate a significant increase in maximum amplitude for $Ca_V1.3$-KO neuronal cultures.

During the period of $Ca_V1.3$-KO data collection, voltage was generated by current output across a resistor to achieve the 20 Hz stimulus. While this voltage was estimated to be around 50 V in magnitude, all other experiments (including **Fig. 3A** and **Fig. 4A**) were performed at a precisely measured 100 V. This adjustment was made to accommodate the observed lack of

response from neuronal cultures (wild-type) to maximum voltage output using the current generator setup in recordings subsequent to the $Ca_V1.3$-KO experiment. The current-resistor method of achieving voltage output was replaced by a battery, which directly outputs voltage of a set value. To ensure the output was consistent with the value set by the battery, we attached an oscilloscope to confirm that the measured voltage at the end of the recording chamber wires matched the indicated battery output. We then performed a voltage titration on spare wild-type neuronal cultures and discovered 100 V to be the optimal voltage for future recordings. This was determined based on the observably similar fluorescent response compared to previous recordings performed with the current-resistor setup. In doing so, we discovered 100 V to be the optimal voltage for future recordings.

The representative time traces of calcium activity depict variability in the wild-type response to the 20 Hz stimulation (**Fig. 3A** and **Fig. 3C**). While this may be in part due to the above-reported inconsistencies in recording conditions, it is not uncommon to observe slight variability in calcium response *in vitro* (see Vierra et al., 2019).

Figure 3

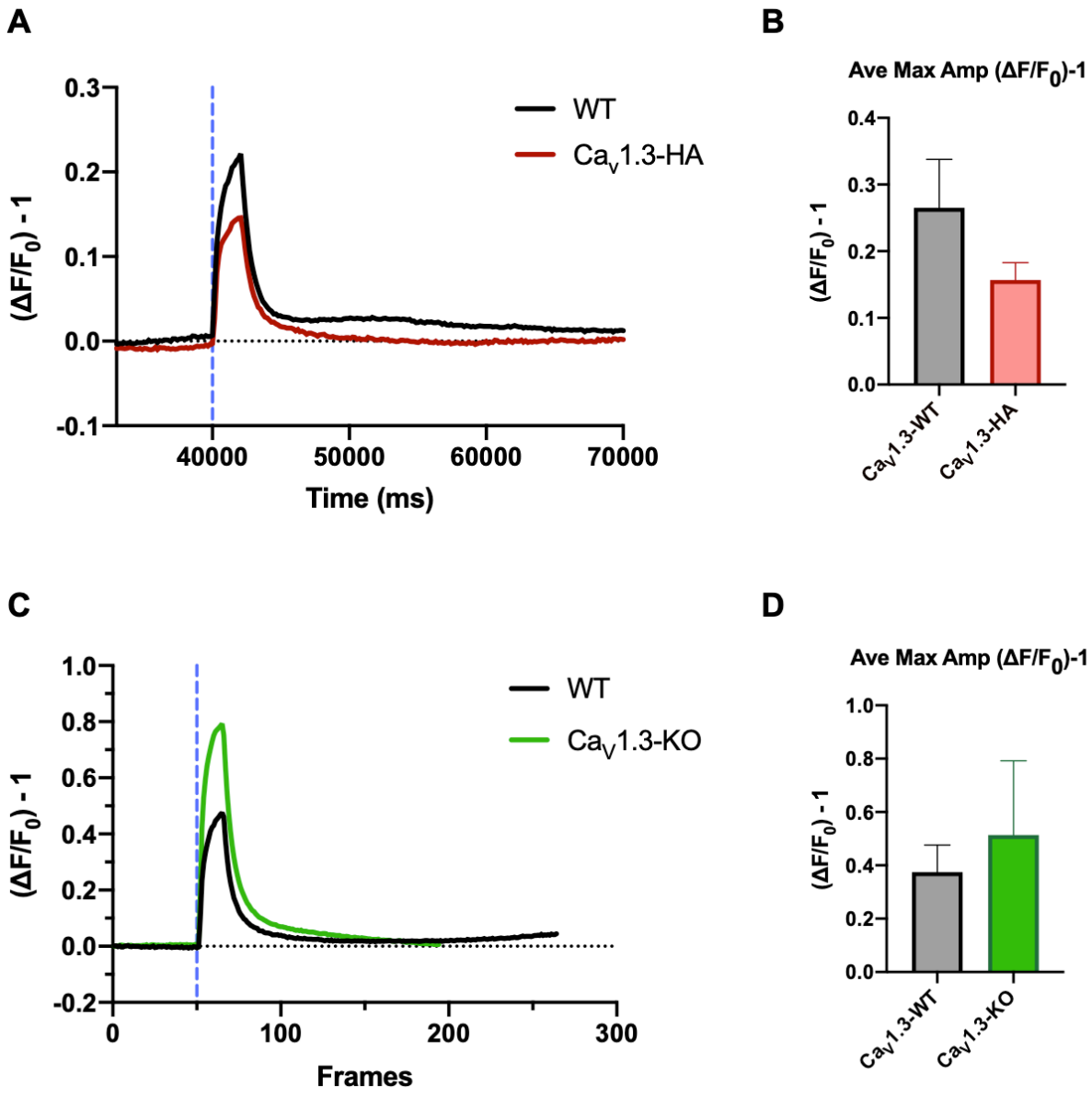

Figure 3. Counterintuitive calcium transients as a result of altered Cav1.3 expression levels. Individual time traces were plotted as the average fluorescence change ((ΔF/F$_0$)-1) for a representative neuronal culture of a given genotype over time. The blue dashed line indicates the 20 Hz (40-pulse) 100 V stimulus introduced at time t=40000 ms. **A,** time trace of a Cav1.3-HA neuronal culture (dark red) compared to WT littermate (black). Data include the following sample sizes (ROIs for an individual culture): Cav1.3-HA, N=61, Ca$_V$1.3-WT (Cav1.3-HA littermates), N=113.

(figure 3 legend continued on next page)

B, comparison of maximum amplitudes for $Ca_V1.3$-WT (N=4 neuronal cultures; mean = 0.2652) vs. $Ca_V1.3$-HA (N=10; mean=0.1569); p=0.0960 (two-tailed *t*-test). **C**, time traces of $Ca_V1.3$-KO neuronal cultures (green) compared to their WT littermates (black). Note the change in $(\Delta F/F_0)$-1 scaling on the y-axis. The x-axis represents frames imaged throughout the recording rather than time, because the acquisition interval was not recorded for this portion of the experiment. Data here include sample sizes (ROIs for an individual culture): $Ca_V1.3$-KO, N=125, $Ca_V1.3$-WT ($Ca_V1.3$-KO littermates), N=120. **D**, comparison of maximum amplitudes for $Ca_V1.3$-WT (N=2 neuronal cultures; mean = 0.3748) vs. $Ca_V1.3$-KO (N=2; mean=0.5140); p=0.0960 (two-tailed *t*-test). Data are represented as mean $\pm$ SEM.

Reciprocal pattern of calcium transients due to manipulated $Ca_V1.2$ expression

We next addressed the effect of genetic manipulations of *Cacna1c* on calcium dynamics. Only effects of $Ca_V1.2$ over-expression were reported, as $Ca_V1.2$-KO mice were allotted to different studies. Upregulation of $Ca_V1.2$ yielded no significant difference in maximum amplitude of calcium response ($p>0.05$; **Fig. 4B**). However, the $Ca_V1.2$-HA trace presented is representative of all samples recorded, and our sample size was limited by the breeding pattern of $Ca_V1.2$-HA mice (**Fig. 4A**; N=3 neuronal cultures). Furthermore, we expect that increasing the sample size of this experiment will exacerbate the trend of decreased maximum amplitude in $Ca_V1.2$-HA.

The calcium activity pattern presented in this experiment was not unexpected, given the striking resemblance of $Ca_V1.2$-HA time traces to previously observed effects of $Ca_V1.3$ over-expression (**Fig. 3A** and **Fig. 3B**). Additionally, both the $Ca_V1.2$-HA and $Ca_V1.3$-HA time traces display calcium responses to a precisely measured 100 V stimulus.

Figure 4

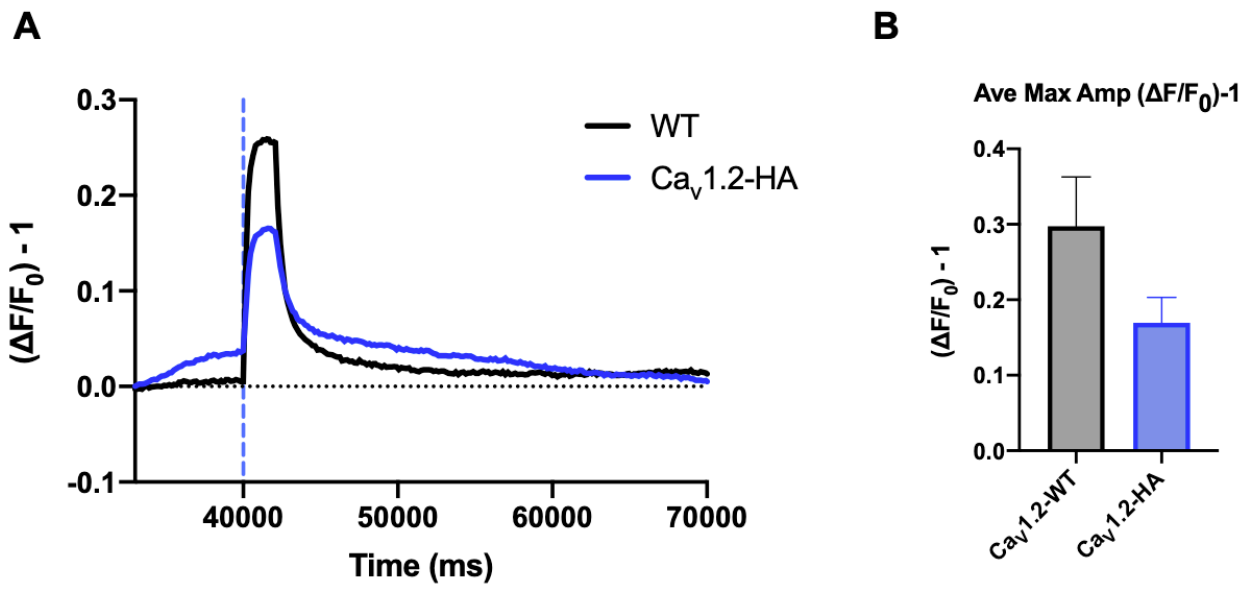

Figure 4. Counterintuitive calcium transients as a result of altered $Ca_V1.2$ expression levels. Individual time traces were plotted as the average fluorescence change ($(\Delta F/F_0)$-1) for a representative neuronal culture of a given genotype over time. The blue dashed line indicates the 20 Hz (40-pulse) stimulus introduced at time t=40000 ms. **A,** time trace of a $Ca_V1.2$-HA neuronal culture (blue) compared to WT littermate (black). Data include the following sample sizes (ROIs for an individual culture): $Ca_V1.2$-HA, N=58, $Ca_V1.2$-WT ($Ca_V1.2$-HA littermates), N=56. **B**, comparison of maximum amplitudes for $Ca_V1.2$-WT (N=3 neuronal cultures; mean = 0.2974) vs. $Ca_V1.2$-HA (N=3; mean=0.1696); p=0.1567 (two-tailed *t*-test). Data are represented as mean ± SEM.

Ca_V1.2 and Ca_V1.3 channels localize in dendrites of hippocampal neuron cultures

To better understand how manipulating expression levels of LVGCCs in mouse neuronal cultures affects calcium dynamics, we used immunocytochemistry (ICC) to spatially map Ca_V1.2 and Ca_V1.3 channels. It has been established that LVGCCs are unique from other VGCCs in that they are most abundantly expressed postsynaptically in neurons of the intact brain (Hell et al., 1993). However, the expression patterns of LVGCCs in neuronal cultures have been less well-defined. This motivated our investigation, as understanding the localization of Ca_V1.2 and Ca_V1.3 in cultured neurons would provide higher spatial resolution for future calcium imaging experiments.

At the time our study was conducted, there were no antibodies specific enough to distinguish between Ca_V1.2 and Ca_V1.3 channels. As such, we used an antibody against the HA epitope of the over-expressed LVGCC transgene. Because HA is used as an over-expression marker in both the Ca_V1.2-HA and Ca_V1.3-HA models, we were only able to study one LVGCC at a time. In conjunction with HA-staining, an antibody against MAP2 was utilized as a dendritic marker. Finally, after double-staining for HA and MAP2 expression, we counter-stained using the nuclear marker DAPI.

Representative images reflect the localization of Ca_V1.2 and Ca_V1.3 to dendrites (**Fig. 5B** and **Fig. 5D**). Colocalization analysis of HA and MAP2 was conducted to generate Pearson's correlation coefficient (PCC). The PCC was calculated using a linear equation to describe the relationship of fluorescent intensity between HA and MAP2 channels (Costes et al., 2004). For this analysis, a p-value above 95% represented significant colocalization of HA with MAP2. In every case, Ca_V1.3-HA and Ca_V1.2-HA images were found to significantly colocalize with MAP2 ($p>95\%$). In all but one case, Ca_V1.2-WT and Ca_V1.3-WT control images failed to demonstrate colocalization between HA and MAP2 ($p<95\%$; **Fig. 5A** and **Fig. 5C**).

While Ca_V1.2-HA and Ca_V1.3-HA colocalized with MAP2, the PCCs for each wild-type control also demonstrated positive correlation. Thus, when statistical comparison was performed between PCCs of over-expressers and wild-type neuron cultures, no significant difference was discovered ($p>0.05$; **Fig. 5E** and **Fig. 5F**). There should have been no observable fluorescence in the HA channel of wild-type images, as only the over-expressed LVGCC transgenes contain the HA epitope. However, we recognize that there were no antibody controls presented in this study;

this was a preliminary experiment, and as such calcium imaging experiments demanded priority of available neuronal cultures.

A source of error is rooted in the the magnification of these images, which appears to be inconsistent. Though the scale-bars were all generated using metadata stored by the confocal microscope, the resolution of these images appear to be variable.

Figure 5

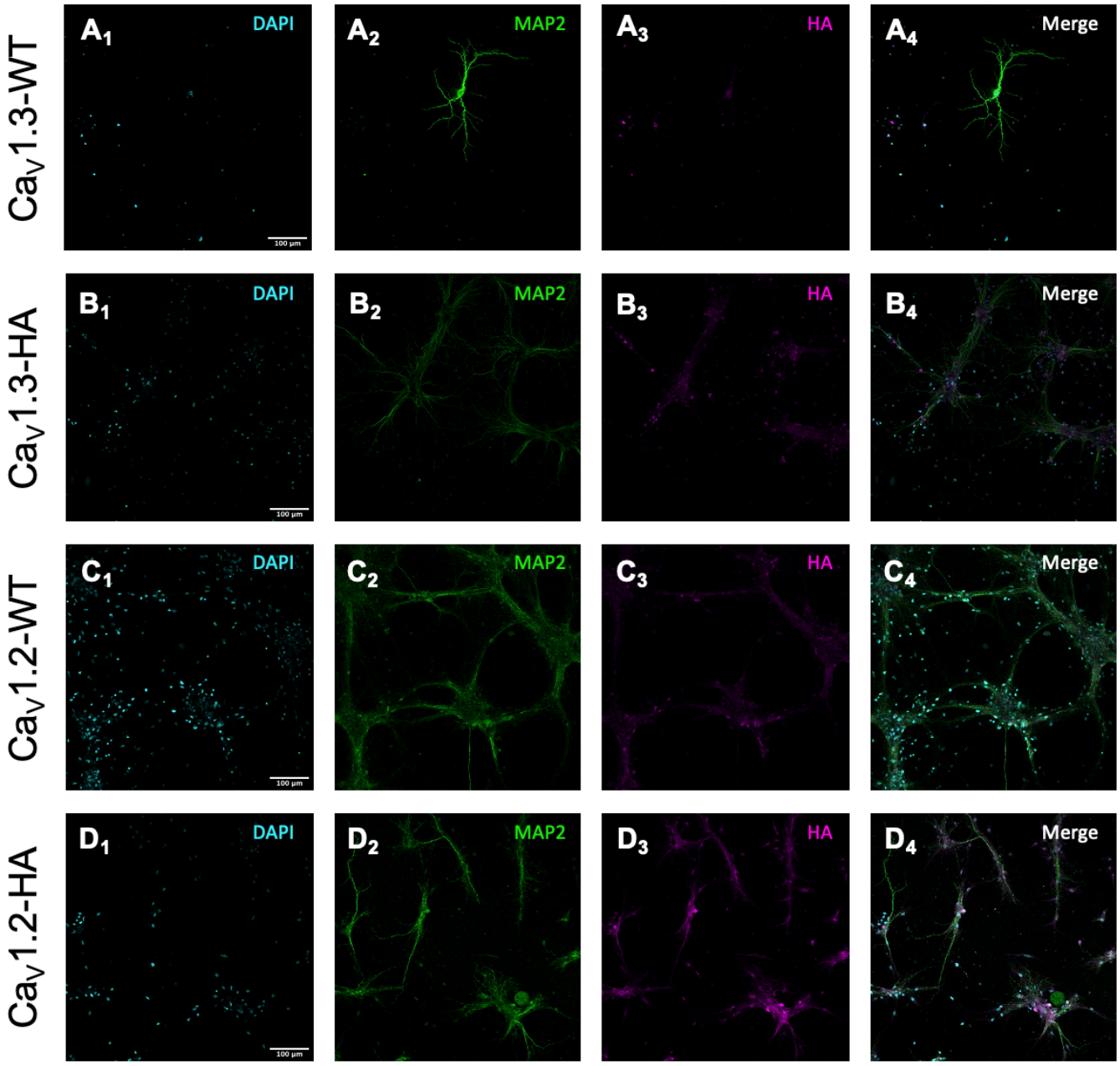

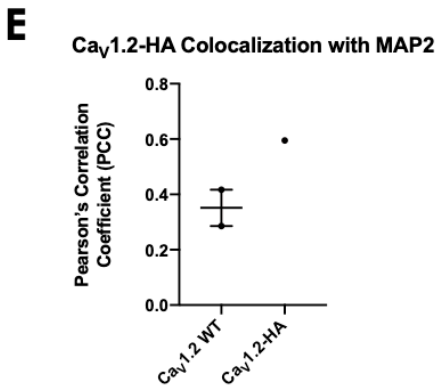

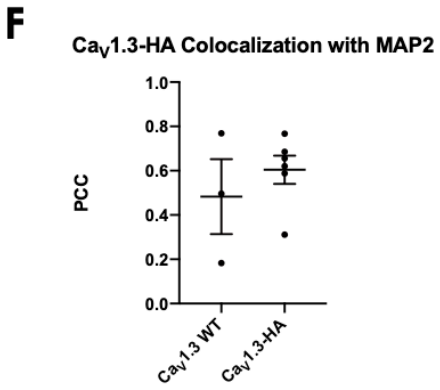

(figure legend on next page)

Figure 5. Immunocytochemical labeling of MAP2 and HA. The MAP2 protein is used as a dendritic marker, while HA immunolabeling shows expression of the respective LVGCC. The merged images in the rightmost column allow for visualization of colocalization between MAP2 and HA. All images were taken at 20× magnification. **A,** $Ca_V1.3$ WT immunolabeling. **B,** $Ca_V1.3$-HA immunolabeling. **C**, $Ca_V1.2$-WT immunolabeling. **D,** $Ca_V1.2$-HA immunolabeling. **E**, Pearson's correlation coefficient (PCC) values of HA and MAP2 immunolabeling in $Ca_V1.2$-WT (N=2) vs. $Ca_V1.2$-HA (N=1). Each point represents a single neuronal culture (p=0.2776; two-tailed *t*-test). **F**, PCC values of HA and MAP2 immunolabeling in $Ca_V1.3$-WT (N=3) vs. $Ca_V1.3$-HA (N=6). Each point represents a single neuronal culture (p=0.4289; two-tailed *t*-test). Data are represented as mean ± SEM. All images presented in this figure were subjected to rolling ball background subtraction and applied a Gaussian Blur of Sigma (radius) = 0.5 after colocalization analysis was performed.

Discussion

In this study, we presented data that work to elucidate the effect of LVGCC genetic manipulations on underlying molecular dynamics. Mutations in $Ca_V1.2$ and $Ca_V1.3$ have been identified as risk alleles for development of neuropsychiatric disorders (Ferreira et al., 2008b; Ross et al., 2016b). Additionally, mutations affecting the *Cacna1c* ($Ca_V1.2$) and *Cacna1d* ($Ca_V1.3$) genes disrupt spatial memory and impair memory consolidation, respectively (McKinney and Murphy, 2006; White et al., 2008). To our knowledge, this is the first set of experiments reporting the effects these genetic manipulations may have on resulting calcium physiology.

Calcium is involved in many biochemical mechanisms throughout the body; thus, even slight deviations in calcium signaling may be detrimental not only to brain function but also overall health. While we have reported no significant differences in the maximum amplitude of calcium transients among the different transgenic LVGCC models in this study, further investigation is warranted. The sample sizes of each experiment were lower than desired, preventing us from making any robust claims. Nonetheless, data consistently pointed towards a reciprocal relationship between expression level and maximum calcium – a measure of overall calcium activity. We believe that increasing the number of neuronal cultures for each genotype would strengthen this trend, potentially enough to yield significance.

As presented in this study, it is best practice to match experimental mice with littermates to eliminate potential confounds of environmental influences. However, it is interesting to note that when all wild-type data ($Ca_V1.3$-WT and $Ca_V1.2$-WT combined) were compared to $Ca_V1.3$-HA, a two-tailed *t*-test revealed significant results ($p=0.0367$). Though controlling for environmental conditions should not be disregarded, this further suggests that there is at least some merit to the counterintuitive calcium activity patterns reported in this study. Consideration must also be given to our definition of individual samples: in the most recent experiments reported (**Fig. 3** and **Fig. 4**), we classified FOVs as samples for amplitude comparison. This differs from our earlier experiment (**Fig. 2**), which defined an individual neuronal cell body as a sample. No statistical analyses were performed on the earlier calcium imaging trial but re-defining our sample size in this way would be a reasonable way to increase the power of our more recent findings. Additionally, this method of reevaluation would allow use to compare data between earlier and more recent trials.

The findings we have reported regarding calcium dynamics only include comparisons of maximum amplitude between neuronal cultures of different genetic backgrounds. Parameters not accounted for in this study include frequency of spontaneous activity and width/area under the curve of calcium transient time traces. Additionally, a longer train of lower-frequency stimulus (such as 0.2 Hz for a 20 second epoch) should be analyzed to more closely mimic physiological conditions in the hippocampus (Dudek and Bear, 1992). Further analysis of these factors is required to more holistically evaluate distortions in LVGCC kinetics.

The variability in the wild-type time traces during calcium imaging experiments remains elusive. There appears to be an intrinsic variability in evoked calcium responses among wild-type cells, likely due to environmental artifacts of neuronal cultures. The fluctuating level of control group responses in this study limits us from drawing any translational implications from genetic manipulation of *Cacna1c* or *Cacna1d*. Other calcium imaging studies focused on LVGCCs have reported maximum amplitudes of wild-type hippocampal neurons between 0.2 – 1.3 ($\Delta F/F_0$) within the same culture (Vierra et al., 2019). Thus, our observation seems to be normative in the field, and we must continue calcium imaging experiments to delineate a standard response.

Despite variability observed among neuronal cultures, the inverse trend of expression level with calcium activity was consistent and merits continued investigation. A subsequent study to confirm or refute our findings in neuronal cultures might include performing calcium imaging experiments on hippocampal slices. Because the expression pattern of LVGCCs are well-characterized in hippocampal circuitry (Hell et al., 1993), we could perform a similar experiment with the substitution of hippocampal slices in replacement of hippocampal neuronal cultures. Recording calcium activity patterns in the intact hippocampus would allow us to explore cell-type specific differences in LVGCC calcium dynamics – a mechanism of high interest in the field of learning and memory. This would be a more representative model of potentially affected calcium dynamics but would considerably compromise the spatial resolution achievable using a neuronal culture model.

The use of a biologically based fluorescent indicator to measure calcium activity is of potential interest for future calcium imaging experiments. Genetically encoded calcium indicators (GECIs), such as GCaMP6f – a commonly used calmodulin (CaM)-dependent fluorescent marker, are commonly used for their high specificity in tracking hippocampal

calcium dynamics (Srinivasan et al., 2015). However, GCaMP6f should not be used as a calcium marker when studying LVGCCs, as this GECI has been recently shown to interfere with $Ca_V1.2$ and $Ca_V1.3$ function (Yang et al., 2018). In their study, *Yang et al.* resolved these issues by developing the GCaMP-X sensor, which has since been successfully used for the study of LVGCC kinetics (Vierra et al., 2019).

We presented data which further define spatial mapping patterns of $Ca_V1.2$ and $Ca_V1.3$ in neuronal cultures. In every case, these LVGCCs localized to dendrites (**Fig. 5A** and **Fig. 5C**). As mentioned previously, we expected not to observe fluorescence in the HA channel for wild-type neuronal cultures. However, we observed a positive PCC correlation for wild-type cultures in each sample. It is possible that the secondary antibodies used in this study were not specific enough to their respective primary antibody host species. In future experiments we plan to include both primary and secondary antibody control images, introduce conjugated antibodies for increased specificity, as well as perform single staining to account for unintentional fluorophore excitation from more than one channel. To further define LVGCC localization in culture, future ICC experiments should incorporate a cell body marker, such as postsynaptic density protein 95 (PSD-95), and a microfilament marker, such as rhodamine phalloidin (F-actin marker).

Another challenge we faced in our ICC experiment was the unavailability of antibodies specific enough to distinguish between $Ca_V1.2$ and $Ca_V1.3$ LVGCCs. To combat this, we targeted the HA epitope of either the $Ca_V1.2$-HA or $Ca_V1.3$-HA mouse model. While this method served the purpose of mapping an individual LVGCC expression pattern, it would be more beneficial to compare spatial mapping of both $Ca_V1.2$ and $Ca_V1.3$ in the same neuronal culture. Due to the lack of antibodies specific enough to achieve this goal, we have considered the generation of a new transgenic mouse line which expresses an endogenous fluorescent marker. Ideally, a useful approach would be to append enhanced green fluorescent protein (EGFP) to the *Cacna1d* gene. This would create the opportunity to analyze expression of $Ca_V1.2$-EGFP, while also allowing for visibility of $Ca_V1.3$-HA in the same culture (assuming the HA antibody used shows specificity). The caveat of this method is that the probability of generating a mouse line containing both LVGCC transgenes is very low, making this a very inefficient and costly process. It would still be useful to have a mouse model containing an endogenous fluorescent marker and no HA epitope, however, as this would yield high specificity of one LVGCC for spatial mapping.

It remains unclear if the hippocampal neuronal culture model in this study maintains $Ca_V1.2$ and $Ca_V1.3$ expression patterns representative of *in-vivo* findings. The ICC experiment presented here only considered transgenic over-expresser mouse models. It is possible that this genetic manipulation results in the addition of LVGCCs into cell regions where they would not normally localize *in vivo*. Furthermore, understanding the localization of $Ca_V1.2$ and $Ca_V1.3$ in neuronal cultures will allow us to verify if neuronal cultures are an accurate model of LVGCC expression patterns. Subsequent calcium imaging studies would then be possible at much higher spatial resolution, as we could narrow our focus to cell region-specific alterations of calcium dynamics.

While the data reported in this study yield no significant differences in calcium dynamics between $Ca_V1.2$ and $Ca_V1.3$ LVGCCs, there is a consistent trend which prompts the consideration of future investigations. The observed decrease in calcium flux upon over-expression of either LVGCC is counterintuitive. Similarly, the reciprocal relationship of LVGCC deletion and increased calcium transients is unexpected. A possible explanation for this pattern could be that genetic manipulations to these LVGCCs may result in a compensatory expression mechanism from the unmanipulated LVGCC. It has been shown that LVGCCs play a role in modulating gene expression (Misra et al., 1994), so it may be possible that there is an underlying cross-talk mechanism in which one LVGCC upregulates in response to deletion of another calcium channel. A protein microarray comparison experiment would serve to elucidate this postulation by measuring protein expression levels of both $Ca_V1.2$ and $Ca_V1.3$ under different genetic backgrounds.

The importance of LVGCCs in physiological mechanisms underlying memory consolidation, development of neuropsychiatric disorders, and general neuronal function has been of great interest to the field in recent years. This study works to further the understanding of $Ca_V1.2$ and $Ca_V1.3$ calcium dynamics, specifically with regards to effects from LVGCC genetic mutations. While the data presented here do not directly establish a link between genetic mutation and altered calcium activity, there is a consistently observed reciprocal trend which demands the attention of future experiments. These LVGCCs are expressed in pathophysiologically relevant neural pathways, and further insight into the underlying molecular dynamics of this circuitry is critical. We have begun spatial characterization of a hippocampal neuronal culture model for altered expression levels of *Cacna1c* and *Cacna1d*. With highly

increased spatial resolution in neuronal cultures, subsequent experiments may shed light on physiological consequences of altered LVGCC gene expression.

References

Alger BE, Nicoll RA (1980) Epileptiform burst afterhyperolarization: calcium-dependent potassium potential in hippocampal CA1 pyramidal cells. Science 210:1122–1124.

Altman J (1963) Autoradiographic investigation of cell proliferation in the brains of rats and cats. Anat Rec 145:573–591.

Ascher P, Nowak L (1987) Electrophysiological studies of NMDA receptors. Trends Neurosci 10:284–288.

Balaji J (2014) Time Series Analyzer V3 Plugin. Available at: https://imagej.nih.gov/ij/plugins/time-series.html [Accessed April 16, 2020].

Bekircan-Kurt CE, Derle Çiftçi E, Kurne AT, Anlar B (2015) Voltage gated calcium channel antibody-related neurological diseases. World J Clin Cases WJCC 3:293–300.

Bhat S, Dao DT, Terrillion CE, Arad M, Smith RJ, Soldatov NM, Gould TD (2012) CACNA1C (Cav1.2) in the pathophysiology of psychiatric disease. Prog Neurobiol 99:1–14.

Biase VD, Obermair GJ, Szabo Z, Altier C, Sanguesa J, Bourinet E, Flucher BE (2008) Stable Membrane Expression of Postsynaptic CaV1.2 Calcium Channel Clusters Is Independent of Interactions with AKAP79/150 and PDZ Proteins. J Neurosci 28:13845–13855.

Bigos KL, Mattay VS, Callicott JH, Straub RE, Vakkalanka R, Kolachana B, Hyde TM, Lipska BK, Kleinman JE, Weinberger DR (2010) Genetic Variation in CACNA1C Affects Brain Circuitries Related to Mental Illness. Arch Gen Psychiatry 67:939.

Boczek NJ, Miller EM, Ye D, Nesterenko VV, Tester DJ, Antzelevitch C, Czosek RJ, Ackerman MJ, Ware SM (2015) Novel Timothy syndrome mutation leading to increase in CACNA1C window current. Heart Rhythm 12:211–219.

Bolte S, Cordelières FP (2006) A guided tour into subcellular colocalization analysis in light microscopy. J Microsc 224:213–232.

Campiglio M, Flucher BE (2015) The Role of Auxiliary Subunits for the Functional Diversity of Voltage-Gated Calcium Channels. J Cell Physiol 230:2019–2031.

Cao Y-Q, Tsien RW (2010) Different Relationship of N- and P/Q-Type Ca2+ Channels to Channel-Interacting Slots in Controlling Neurotransmission at Cultured Hippocampal Synapses. J Neurosci 30:4536–4546.

Carbone E, Calorio C, Vandael DHF (2014) T-type channel-mediated neurotransmitter release. Pflugers Arch 466:677–687.

Catterall WA (2011) Voltage-Gated Calcium Channels. Cold Spring Harb Perspect Biol 3 Available at: https://www.ncbi.nlm.nih.gov/pmc/articles/PMC3140680/ [Accessed April 15, 2020].

Clapham DE (2007) Calcium Signaling. Cell 131:1047–1058.

Costes SV, Daelemans D, Cho EH, Dobbin Z, Pavlakis G, Lockett S (2004) Automatic and Quantitative Measurement of Protein-Protein Colocalization in Live Cells. Biophys J 86:3993–4003.

Crow JF (2002) Unequal by Nature: A Geneticist's Perspective on Human Differences. Daedalus 131:81–88.

Davies A, Douglas L, Hendrich J, Wratten J, Tran Van Minh A, Foucault I, Koch D, Pratt WS, Saibil HR, Dolphin AC (2006) The calcium channel alpha2delta-2 subunit partitions with CaV2.1 into lipid rafts in cerebellum: implications for localization and function. J Neurosci Off J Soc Neurosci 26:8748–8757.

Deisseroth K, Bito H, Tsien RW (1996) Signaling from Synapse to Nucleus: Postsynaptic CREB Phosphorylation during Multiple Forms of Hippocampal Synaptic Plasticity. Neuron 16:89–101.

Deisseroth K, Heist EK, Tsien RW (1998) Translocation of calmodulin to the nucleus supports CREB phosphorylation in hippocampal neurons. Nature 392:198–202.

Disterhoft JF, Thompson LT, Moyer JR, Mogul DJ (1996) Calcium-dependent afterhyperpolarization and learning in young and aging hippocampus. Life Sci 59:413–420.

Dolphin AC (2016) Voltage-gated calcium channels and their auxiliary subunits: physiology and pathophysiology and pharmacology. J Physiol 594:5369–5390.

Dudek SM, Bear MF (1992) Homosynaptic long-term depression in area CA1 of hippocampus and effects of N-methyl-D-aspartate receptor blockade. Proc Natl Acad Sci U S A 89:4363–4367.

Ertel EA, Campbell KP, Harpold MM, Hofmann F, Mori Y, Perez-Reyes E, Schwartz A, Snutch TP, Tanabe T, Birnbaumer L, Tsien RW, Catterall WA (2000) Nomenclature of Voltage-Gated Calcium Channels. Neuron 25:533–535.

Ferreira MAR et al. (2008a) Collaborative genome-wide association analysis supports a role for ANK3 and CACNA1C in bipolar disorder. Nat Genet 40:1056–1058.

Ferreira MAR et al. (2008b) Collaborative genome-wide association analysis supports a role for ANK3 and CACNA1C in bipolar disorder. Nat Genet 40:1056–1058.

Folstein S, Rutter M (1977) Genetic influences and infantile autism. Nature 265:726–728.

Gamelli AE, McKinney BC, White JA, Murphy GG (2011) Deletion of the L-type calcium channel CaV1.3 but not CaV1.2 results in a diminished sAHP in mouse CA1 pyramidal neurons. Hippocampus 21:133–141.

Glynn MW, McAllister AK (2006) Immunocytochemistry and quantification of protein colocalization in cultured neurons. Nat Protoc 1:1287–1296.

Gusella JF, Wexler NS, Conneally PM, Naylor SL, Anderson MA, Tanzi RE, Watkins PC, Ottina K, Wallace MR, Sakaguchi AY (1983) A polymorphic DNA marker genetically linked to Huntington's disease. Nature 306:234–238.

Hell JW, Westenbroek RE, Warner C, Ahlijanian MK, Prystay W, Gilbert MM, Snutch TP, Catterall WA (1993) Identification and differential subcellular localization of the neuronal class C and class D L-type calcium channel alpha 1 subunits. J Cell Biol 123:949–962.

Helton TD, Xu W, Lipscombe D (2005) Neuronal L-Type Calcium Channels Open Quickly and Are Inhibited Slowly. J Neurosci 25:10247–10251.

Hetzenauer A, Sinnegger-Brauns MJ, Striessnig J, Singewald N (2006) Brain activation pattern induced by stimulation of L-type Ca2+-channels: Contribution of CaV1.3 and CaV1.2 isoforms. Neuroscience 139:1005–1015.

Jenkins MA, Christel CJ, Jiao Y, Abiria S, Kim KY, Usachev YM, Obermair GJ, Colbran RJ, Lee A (2010) Ca2+-Dependent Facilitation of Cav1.3 Ca2+ Channels by Densin and Ca2+/Calmodulin-Dependent Protein Kinase II. J Neurosci 30:5125–5135.

Josephson IR, Varadi G (1996) The beta subunit increases Ca2+ currents and gating charge movements of human cardiac L-type Ca2+ channels. Biophys J 70:1285–1293.

Krueger JN, Moore SJ, Parent R, McKinney BC, Lee A, Murphy GG (2017) A novel mouse model of the aged brain: Over-expression of the L-type voltage-gated calcium channel Ca V 1.3. Behav Brain Res 322:241–249.

Lancaster B, Nicoll RA (1987) Properties of two calcium-activated hyperpolarizations in rat hippocampal neurones. J Physiol 389:187–203.

Liu M-G, Li H, Xu X, Barnstable CJ, Zhang SS-M (2008) Comparison of gene expression during in vivo and in vitro postnatal retina development. J Ocul Biol Dis Infor 1:59–72.

Llinás RR, Sugimori M, Cherksey B (1989) Voltage-Dependent Calcium Conductances in Mammalian Neurons. Ann N Y Acad Sci 560:103–111.

MacDonald ME et al. (1993) A novel gene containing a trinucleotide repeat that is expanded and unstable on Huntington's disease chromosomes. Cell 72:971–983.

McGuffin P, Farmer AE, Gottesman II, Murray RM, Reveley AM (1984) Twin concordance for operationally defined schizophrenia. Confirmation of familiality and heritability. Arch Gen Psychiatry 41:541–545.

McGuffin P, Rijsdijk F, Andrew M, Sham P, Katz R, Cardno A (2003) The heritability of bipolar affective disorder and the genetic relationship to unipolar depression. Arch Gen Psychiatry 60:497–502.

McKinney BC, Murphy GG (2006) The L-Type voltage-gated calcium channel Cav1.3 mediates consolidation, but not extinction, of contextually conditioned fear in mice. Learn Mem 13:584–589.

Mermelstein PG, Bito H, Deisseroth K, Tsien RW (2000) Critical Dependence of cAMP Response Element-Binding Protein Phosphorylation on L-Type Calcium Channels Supports a Selective Response to EPSPs in Preference to Action Potentials. J Neurosci 20:266–273.

Misra RP, Bonni A, Miranti CK, Rivera VM, Sheng M, Greenberg ME (1994) L-type voltage-sensitive calcium channel activation stimulates gene expression by a serum response factor-dependent pathway. J Biol Chem 269:25483–25493.

Moldovean SN, Chiş V (2020) Molecular Dynamics Simulations Applied to Structural and Dynamical Transitions of the Huntingtin Protein: A Review. ACS Chem Neurosci 11:105–120.

Moyer JR, Thompson LT, Disterhoft JF (1996) Trace Eyeblink Conditioning Increases CA1 Excitability in a Transient and Learning-Specific Manner. J Neurosci 16:5536–5546.

Murphy GG, Fedorov NB, Giese KP, Ohno M, Friedman E, Chen R, Silva AJ (2004) Increased Neuronal Excitability, Synaptic Plasticity, and Learning in Aged Kvβ1.1 Knockout Mice. Curr Biol 14:1907–1915.

Murphy GG, Shah V, Hell JW, Silva AJ (2006) Investigation of age-related cognitive decline using mice as a model system: neurophysiological correlates. Am J Geriatr Psychiatry Off J Am Assoc Geriatr Psychiatry 14:1012–1021.

Myrick LK, Deng P-Y, Hashimoto H, Oh YM, Cho Y, Poidevin MJ, Suhl JA, Visootsak J, Cavalli V, Jin P, Cheng X, Warren ST, Klyachko VA (2015) Independent role for presynaptic FMRP revealed by an *FMR1* missense mutation associated with intellectual disability and seizures. Proc Natl Acad Sci 112:949–956.

Neely A, Wei X, Olcese R, Birnbaumer L, Stefani E (1993) Potentiation by the beta subunit of the ratio of the ionic current to the charge movement in the cardiac calcium channel. Science 262:575–578.

Ozaki K, Ohnishi Y, Iida A, Sekine A, Yamada R, Tsunoda T, Sato H, Sato H, Hori M, Nakamura Y, Tanaka T (2002) Functional SNPs in the lymphotoxin-α gene that are associated with susceptibility to myocardial infarction. Nat Genet 32:650–654.

Perkowski JJ, Murphy GG (2011) Deletion of the Mouse Homolog of KCNAB2, a Gene Linked to Monosomy 1p36, Results in Associative Memory Impairments and Amygdala Hyperexcitability. J Neurosci 31:46–54.

Platzer J, Engel J, Schrott-Fischer A, Stephan K, Bova S, Chen H, Zheng H, Striessnig J (2000) Congenital deafness and sinoatrial node dysfunction in mice lacking class D L-type Ca2+ channels. Cell 102:89–97.

Rajadhyaksha AM, Kosofsky BE (2005) Psychostimulants, L-type Calcium Channels, Kinases, and Phosphatases. Neurosci Rev J Bringing Neurobiol Neurol Psychiatry 11:494–502.

Randall A, Tsien RW (1995) Pharmacological dissection of multiple types of Ca2+ channel currents in rat cerebellar granule neurons. J Neurosci Off J Soc Neurosci 15:2995–3012.

Rosati B, Yan Q, Lee MS, Liou S-R, Ingalls B, Foell J, Kamp TJ, McKinnon D (2011) Robust L-type calcium current expression following heterozygous knockout of the Cav1.2 gene in adult mouse heart. J Physiol 589:3275–3288.

Ross J, Gedvilaite E, Badner JA, Erdman C, Baird L, Matsunami N, Leppert M, Xing J, Byerley W (2016a) A Rare Variant in ***CACNA1D*** Segregates with 7 Bipolar I Disorder Cases in a Large Pedigree. Mol Neuropsychiatry 2:145–150.

Ross J, Gedvilaite E, Badner JA, Erdman C, Baird L, Matsunami N, Leppert M, Xing J, Byerley W (2016b) A Rare Variant in CACNA1D Segregates with 7 Bipolar I Disorder Cases in a Large Pedigree. Mol Neuropsychiatry 2:145–150.

Shimomura O, Johnson FH, Saiga Y (1962) Extraction, purification and properties of aequorin, a bioluminescent protein from the luminous hydromedusan, Aequorea. J Cell Comp Physiol 59:223–239.

Smoller JW, Kendler K, Craddock N (2013) Identification of risk loci with shared effects on five major psychiatric disorders: a genome-wide analysis. Lancet 381:1371–1379.

Splawski I, Timothy KW, Sharpe LM, Decher N, Kumar P, Bloise R, Napolitano C, Schwartz PJ, Joseph RM, Condouris K, Tager-Flusberg H, Priori SG, Sanguinetti MC, Keating MT (2004) CaV1.2 Calcium Channel Dysfunction Causes a Multisystem Disorder Including Arrhythmia and Autism. Cell 119:19–31.

Srinivasan R, Huang BS, Venugopal S, Johnston AD, Chai H, Zeng H, Golshani P, Khakh BS (2015) Ca 2+ signaling in astrocytes from Ip3r2 −/− mice in brain slices and during startle responses in vivo. Nat Neurosci 18:708–717.

Storm JF (1987) Action potential repolarization and a fast after-hyperpolarization in rat hippocampal pyramidal cells. J Physiol 385:733–759.

Storm JF (1990) Potassium currents in hippocampal pyramidal cells. Prog Brain Res 83:161–187.

Striessnig J, Bolz HJ, Koschak A (2010) Channelopathies in Cav1.1, Cav1.3, and Cav1.4 voltage-gated L-type Ca2+ channels. Pflugers Arch 460:361.

Takahashi M, Seagar MJ, Jones JF, Reber BF, Catterall WA (1987) Subunit structure of dihydropyridine-sensitive calcium channels from skeletal muscle. Proc Natl Acad Sci U S A 84:5478–5482.

Tanabe T, Takeshima H, Mikami A, Flockerzi V, Takahashi H, Kangawa K, Kojima M, Matsuo H, Hirose T, Numa S (1987) Primary structure of the receptor for calcium channel blockers from skeletal muscle. Nature 328:313–318.

Temme SJ, Bell RZ, Fisher GL, Murphy GG (2016) Deletion of the Mouse Homolog of CACNA1C Disrupts Discrete Forms of Hippocampal-Dependent Memory and Neurogenesis within the Dentate Gyrus. eNeuro 3.

Temme SJ, Murphy GG (2017) The L-type voltage-gated calcium channel Ca v 1.2 mediates fear extinction and modulates synaptic tone in the lateral amygdala. Learn Mem 24:580–588.

Toda T, Parylak SL, Linker SB, Gage FH (2019) The role of adult hippocampal neurogenesis in brain health and disease. Mol Psychiatry 24:67–87.

Vierra NC, Kirmiz M, van der List D, Santana LF, Trimmer JS (2019) Kv2.1 mediates spatial and functional coupling of L-type calcium channels and ryanodine receptors in mammalian neurons Swartz KJ, Marder E, eds. eLife 8:e49953.

White JA, McKinney BC, John MC, Powers PA, Kamp TJ, Murphy GG (2008) Conditional forebrain deletion of the L-type calcium channel CaV1.2 disrupts remote spatial memories in mice. Learn Mem 15:1–5.

Yang Y, Liu N, He Y, Liu Y, Ge L, Zou L, Song S, Xiong W, Liu X (2018) Improved calcium sensor GCaMP-X overcomes the calcium channel perturbations induced by the calmodulin in GCaMP. Nat Commun 9:1–18.

Zhu Y, Romero MI, Ghosh P, Ye Z, Charnay P, Rushing EJ, Marth JD, Parada LF (2001) Ablation of NF1 function in neurons induces abnormal development of cerebral cortex and reactive gliosis in the brain. Genes Dev 15:859–876.